

Heavy Flavor Baryons at the Tevatron

Thomas Kuhr¹ on behalf of the CDF and D0 Collaborations
Karlsruhe Institute of Technology
Institut für Experimentelle Kernphysik
Wolfgang-Gaede-Str. 1
D-76131 Karlsruhe, GERMANY

The Tevatron experiments CDF and D0 have filled many empty spots in the spectrum of heavy baryons over the last few years. The most recent results are described in this article: The first direct observation of the Ξ_b^0 , improved measurements of Σ_b properties, a new measurement of the $\Lambda_b \rightarrow J/\psi \Lambda$ branching ratio, and a high-statistics study of charm baryons.

1 Introduction

The Λ_b baryon, with quark content $|udb\rangle$, is known since about 20 years. But only recently considerable progress could be made on the other components of the b -baryon family by the Tevatron experiments CDF and D0. The charged Σ_b baryons ($|uub\rangle$ and $|ddb\rangle$) were observed in the decay to $\Lambda_b \pi^\pm$ by CDF in 2007 [1]. In the same year the charged Ξ_b state ($|dsb\rangle$) was directly observed by D0 [2] and CDF [3] in the decay to $J/\psi \Xi^-$. Until then only indirect observations of the Ξ_b via an excess in $\Xi^- \ell^-$ events were reported by the ALEPH [4] and DELPHI [5] experiments. In 2008 the Ω_b^- ($|ssb\rangle$) was discovered by D0 in the decay to $J/\psi \Omega^-$ [6]. CDF observed the Ω_b^- briefly afterwards [7], but measured a mass that is incompatible with the value quoted by D0. In the last year the Tevatron experiments continued to improve the knowledge about heavy baryons by further measurements, which are presented in this article.

The progress on the field of heavy baryons has been possible because of the large dataset delivered by the Tevatron $p\bar{p}$ collider running at a center of mass energy of $\sqrt{s} = 1.96$ TeV. During the Run II period, both experiments, CDF and D0, collected about 10 fb^{-1} of data. The Tevatron is well suited for heavy baryon studies, e.g. compared to B factories, because all kinds of heavy hadrons are produced with significant cross section. On the other hand the high combinatorial background and the huge inelastic cross section are a challenge. To be able to record the interesting events with heavy flavor hadrons, highly selective and

¹Thomas.Kuhr@kit.edu

efficient triggers are essential [8]. Both experiments can trigger on dimuon pairs so that heavy baryon decays to J/ψ mesons can be studied. While D0 has an efficient single muon trigger, CDF is able to trigger on hadronic decays of heavy hadrons identified by tracks displaced from the primary vertex.

2 Ξ_b^0 Observation

The Ξ_b^- was directly observed by D0 and CDF in the decay to $J/\psi \Xi^-$. The events were triggered by the dimuon decay of the J/ψ and the Ξ^- was reconstructed via $\Xi^- \rightarrow \Lambda \pi^-$. Since the corresponding decay of the neutral isospin partner, $\Xi_b^0 (|usb\rangle) \rightarrow J/\psi \Xi^0$ with $\Xi^0 \rightarrow \Lambda \pi^0$, involves a neutral pion which cannot be detected efficiently, a search for the Ξ_b^0 requires a trigger on a hadronic decay. CDF reported the first observation of the Ξ_b^0 [9] in the decay chain $\Xi_b^0 \rightarrow \Xi_c^+ \pi^-$, $\Xi_c^+ \rightarrow \Xi^- \pi^+ \pi^+$, and $\Xi^- \rightarrow \Lambda \pi^-$ briefly after the Hadron2011 conference and therefore this result is included in this article although it was not shown at the conference. In the same analysis of 4.2 fb^{-1} of data, CDF also confirms the observation of the Ξ_b^- baryon, reconstructed for the first time in its hadronic final state $\Xi_c^0 \pi^-$ with $\Xi_c^0 \rightarrow \Xi^- \pi^+$.

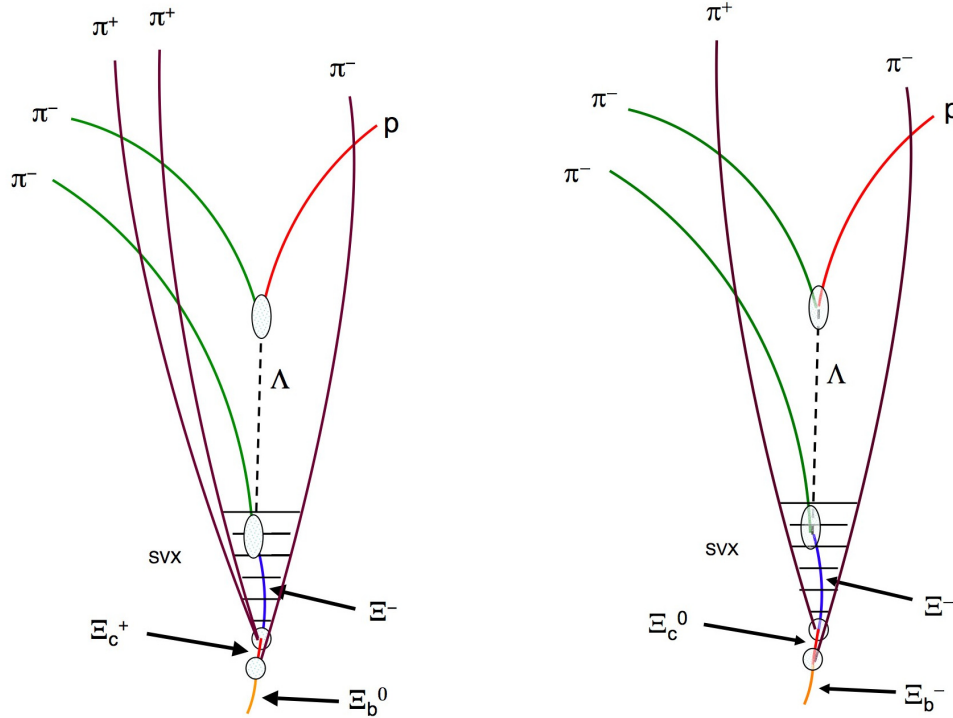


Figure 1: Illustration of the Ξ_b^0 (left) and Ξ_b^- (right) decay topology.

The reconstruction starts with the selection of Λ candidates from $p\pi^-$ pairs. Ξ^- candidates are constructed from $\Lambda\pi^-$ pairs which are then combined with one or two π^+ tracks to form Ξ_c^0 or Ξ_c^+ candidates, respectively. The addition of a further π^- track to the Ξ_c baryons yields the Ξ_b candidates. A schematic illustration of the reconstructed decay chain is shown in Fig. 1.

The long lifetime of hyperons and charm baryons is exploited by requirements on the reconstructed flight lengths, decay times, or impact parameters. The Ξ^- candidate is required to be identified by hits in the silicon vertex detector (SVX) which significantly reduces background as illustrated in Fig. 2. A simultaneous vertex fit of all tracks with mass constraints for the Λ , Ξ^- , and Ξ_c is performed to improve the momentum resolution of the Ξ_b . The reconstructed invariant mass spectra of Ξ_b candidates are shown in Fig. 3.

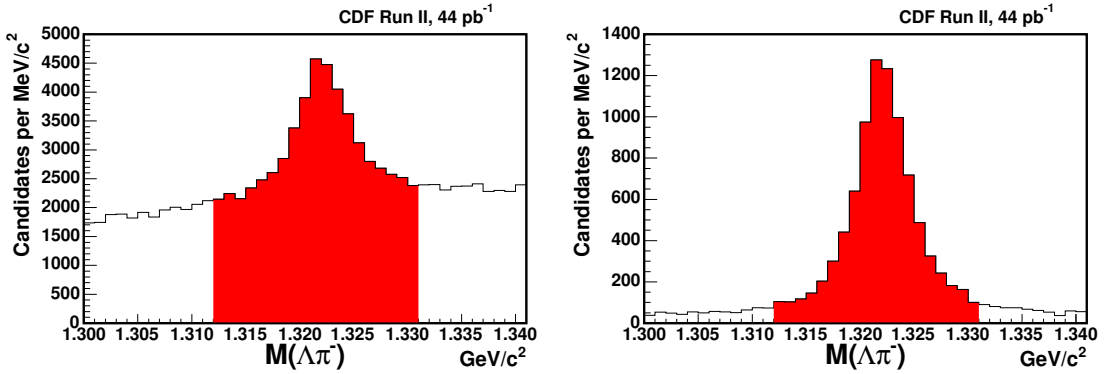


Figure 2: The invariant mass distributions of Ξ_b^- candidates without (left) and with (right) the requirement of SVX hits.

A clear signal is evident for the Ξ_b^- and Ξ_b^0 . To determine the significance and to measure the mass of the states, an unbinned likelihood fit is performed. The signal is described by a Gaussian and the background by a linear function. The width of the Gaussian is given by the reconstructed mass resolution of each candidate multiplied with a common scale factor which is fitted to a value consistent with 1. The significance is determined from a likelihood ratio to be at least 6.8σ . The yields are $25.8^{+5.5}_{-5.2} \Xi_b^-$ and $25.3^{+5.6}_{-5.4} \Xi_b^0$ baryons. Their masses are measured to be $m(\Xi_b^-) = (5796.7 \pm 5.1 \pm 1.4) \text{ GeV}/c^2$ and $m(\Xi_b^0) = (5787.8 \pm 5.0 \pm 1.3) \text{ GeV}/c^2$. The systematic uncertainties are given by the absolute mass scale, the mass resolution scale, and the world average Ξ_c masses. The Ξ_b^- mass is well consistent with the one measured in the $J/\psi\Xi^-$ decay channel [3].

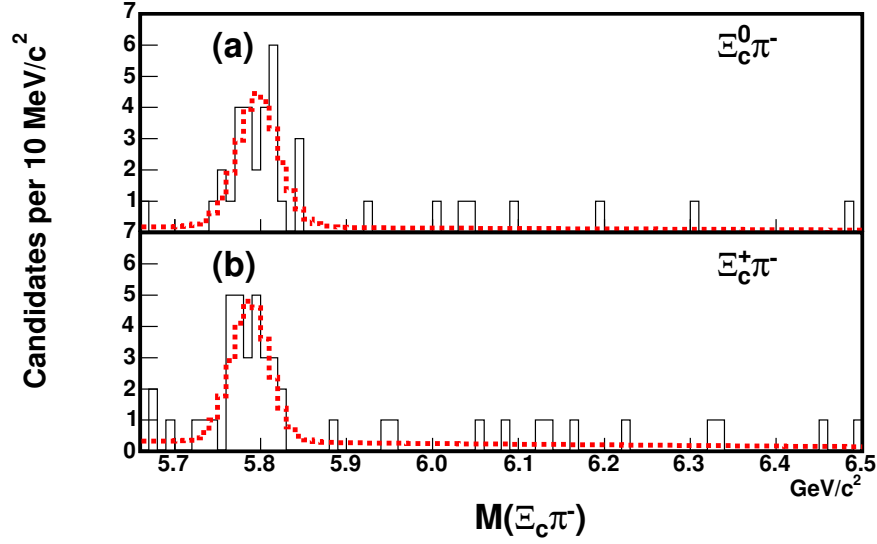


Figure 3: The $\Xi_c^0 \pi^-$ (a) and $\Xi_c^+ \pi^-$ (b) mass distributions with fit projection as dashed line.

3 $\Sigma_b^{(*)}$ Masses and Widths

$\Sigma_b^{(*)}$ baryons form an isospin triplet and have a flavor symmetric light di-quark with spin 1. This couples with the heavy quark spin to two possible spin states, $J^P = \frac{1}{2}^+$ and $J^P = \frac{3}{2}^+$, referred to as Σ_b and Σ_b^* , respectively. The $\Sigma_b^{(*)}$ baryons decay strongly to the Λ_b ground state via the emission of a pion. Figure 4 illustrates the spectrum of baryons consisting of u , d , and one b quark.

The decays of the charged $\Sigma_b^{(*)}$ states were first observed by CDF in 2007 [1]. In a data sample of 1.1 fb^{-1} , the significance of each of the four states was about 3σ . Assuming the same hyperfine splitting between Σ_b^* and Σ_b for both charged states, the masses were measured. Now CDF presented an updated analysis of 6 fb^{-1} of data with improved significances, unconstrained mass measurements, and first measurements of the $\Sigma_b^{(*)}$ natural widths [10].

The Λ_b baryons from the $\Sigma_b^{(*)} \rightarrow \Lambda_b \pi^\pm$ decay are reconstructed in the decay to $\Lambda_c^+ \pi^-$ with $\Lambda_c^+ \rightarrow p K^- \pi^+$. The tracks of the final state particles from the Λ_c^+ and Λ_b decay are usually displaced from the primary vertex so that these decays are selected by the hadronic trigger. The selection requirements on lifetime and kinematic variables are optimized on the significance of the Λ_b signal. The reconstructed Λ_b invariant mass distribution is shown in Fig. 5. The selected sample contains 16 000 Λ_b baryons with a signal to background ratio

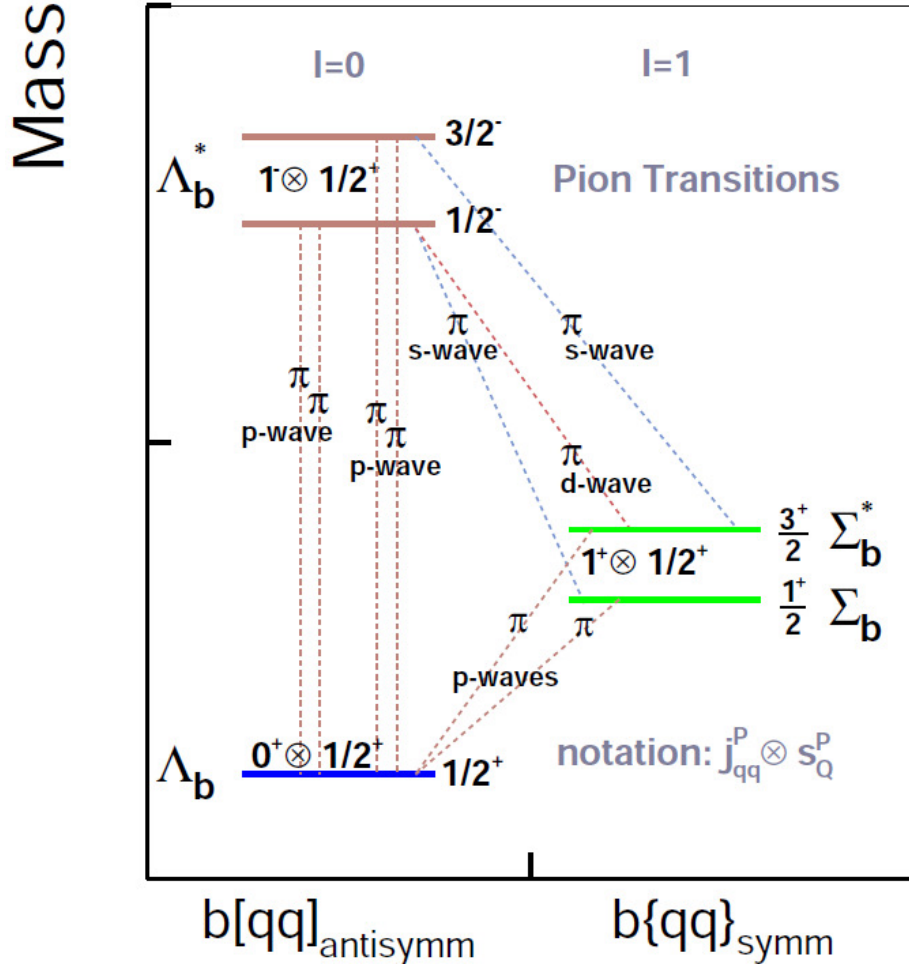


Figure 4: Spectrum and decays of b baryons with no strangeness.

of about 1.8. Thus the main background to the $\Sigma_b^{(*)}$ signals in $\Lambda_b \pi^\pm$ combinations are real Λ_b with a random pion.

To measure masses and width, the Q value distribution is fitted, where Q is the difference between the reconstructed $\Lambda_b \pi^\pm$ mass and the sum of Λ_b and pion masses. The background is described by an empirical function consisting of a second order polynomial times a square root function to describe the threshold behavior. Compared to the previous analysis, the background description does not rely on simulation any more. Each of the four signal peaks is parametrized by a non-relativistic Breit-Wigner. To account for the p wave decay, a variable width is used which scales with p_π^3 where p_π is the pion momentum in the $\Sigma_b^{(*)}$ rest frame. The natural line shape is convolved with a double Gaussian resolution function whose parameters are determined from simulation. Projections of the fit are shown in Fig. 6.

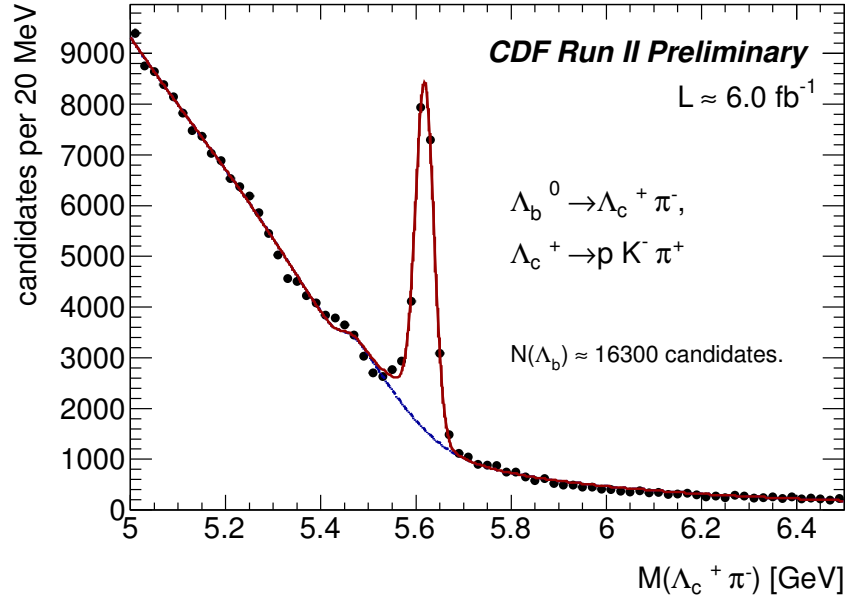


Figure 5: Invariant mass distribution of Λ_b candidates.

The hypotheses of having two, one, or no signal peaks are compared using a likelihood ratio. For both isospin states the hypothesis of two peaks is favored by more than 7σ over any of the other hypotheses, meaning that each peak has a significance above 7σ .

The measured masses and width are quoted in Tab. 1. The dominant systematic uncertainty for the Q values is the uncertainty on the momentum scale which is estimated from the comparison of reconstructed Σ_c^{++} , Σ_c^0 , Λ_c^{*+} , and D^{*+} masses with world average values. The systematic uncertainty of the widths is dominated by the uncertainty on the resolution model estimated from $D^{*+} \rightarrow D^0 \pi^+$ decays. Further considered sources of systematic uncertainties are the background model and a fit bias. When absolute masses are calculated from the Q values the systematic uncertainty is limited by the knowledge of the Λ_b mass.

Compared with the previous analysis, the mass measurements are improved in precision by at least a factor two. The isospin splittings and the natural widths are measured for the first time.

4 $\Lambda_b \rightarrow J/\psi \Lambda$ Branching Ratio

The quark level transition $b \rightarrow s$ is a flavor changing neutral current process and thus forbidden at tree level in the standard model and therefore considered a sensitive probe for new physics. While such processes are well studied for B mesons, little is known about

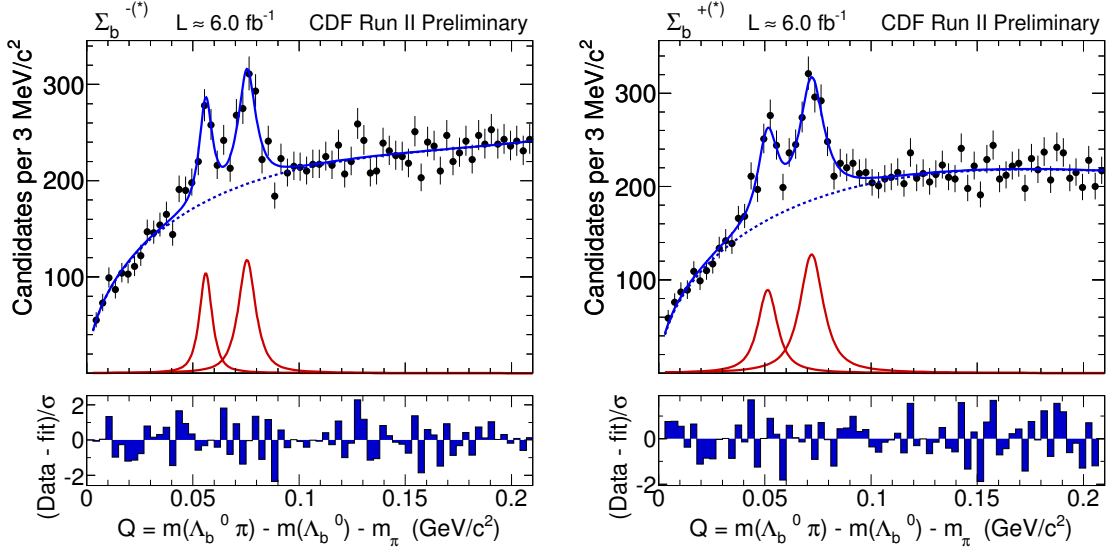


Figure 6: Q value distribution of $\Sigma_b^{(*)+}$ (left) and $\Sigma_b^{(*)-}$ (right) candidates.

$b \rightarrow s$ transitions in baryons. The decay $\Lambda_b \rightarrow J/\psi \Lambda$ is kinematically very similar to the flavor changing neutral current decay $\Lambda_b \rightarrow \mu^+ \mu^- \Lambda$ and was first observed by CDF in Run I [11]. However, the measured value of the Λ_b production fraction times branching ratio, $f(b \rightarrow \Lambda_b) \mathcal{B}(\Lambda_b \rightarrow J/\psi \Lambda) = (4.7 \pm 2.3 \text{ (stat.)} \pm 0.2 \text{ (syst.)}) \times 10^{-5}$ has large uncertainties.

The D0 experiment presented a new measurement of this quantity using a data sample of 6.1 fb^{-1} selected by a dimuon trigger [12]. The Λ and Λ_b daughter particles are fitted to a vertex, respectively, and requirements on momenta, impact parameters and decay times are imposed that are optimized on the signal significance as estimated from simulation and data sidebands. Cascade decays like $\Sigma \rightarrow \Lambda \gamma$ or $\Xi^0 \rightarrow \Lambda \pi^0$ are suppressed by requiring that the direction from the primary to the Λ decay vertex coincides with the Λ momentum direction.

Kinematically very similar $B^0 \rightarrow J/\psi K_S^0$ decays with $K_S^0 \rightarrow \pi^+ \pi^-$ are used as normalization channel. Figure 7 shows the invariant mass distributions of Λ_b and B^0 candidates with a fit of a double Gaussian for signal and a second order polynomial for background.

Taking the relative efficiency from simulation, the following relative cross section is measured:

$$\sigma_{rel} = \frac{f(b \rightarrow \Lambda_b) \mathcal{B}(\Lambda_b \rightarrow J/\psi \Lambda)}{f(b \rightarrow B^0) \mathcal{B}(B^0 \rightarrow J/\psi K_S^0)} = 0.345 \pm 0.034 \text{ (stat.)} \pm 0.033 \text{ (syst.)} \pm 0.003 \text{ (PDG)}.$$

The dominant systematic uncertainty comes from the unknown Λ_b polarization, followed by the uncertainty due to the fit model. The uncertainties on the relative efficiency and the cross-feed fractions have no significant influence. Several cross checks were performed to

State	Q value [MeV/ c^2]	Mass [MeV/ c^2]	Width [MeV/ c^2]	Yield
Σ_b^+	$52.0^{+0.9+0.09}_{-0.8-0.4}$	$5811.2^{+0.9}_{-0.8} \pm 1.7$	$9.2^{+3.8+1.0}_{-2.9-1.1}$	$468^{+110+18}_{-95-15}$
Σ_b^-	$56.2^{+0.6+0.07}_{-0.5-0.4}$	$5815.5^{+0.6}_{-0.5} \pm 1.7$	$4.3^{+3.1+1.0}_{-2.1-1.1}$	$333^{+93}_{-73} \pm 35$
Σ_b^{*+}	$72.7 \pm 0.7^{+0.12}_{-0.6}$	$5832.0 \pm 0.7 \pm 1.8$	$10.4^{+2.7+0.8}_{-2.2-1.2}$	$782^{+114+25}_{-103-27}$
Σ_b^{*-}	$75.7 \pm 0.6^{+0.08}_{-0.6}$	$5835.0 \pm 0.6 \pm 1.8$	$6.4^{+2.2+0.7}_{-1.8-1.1}$	$522^{+85}_{-76} \pm 29$

Isospin splitting [MeV/ c^2]	
$m(\Sigma_b^+) - m(\Sigma_b^-)$	$-4.2^{+1.1+0.07}_{-0.9-0.09}$
$m(\Sigma_b^{*+}) - m(\Sigma_b^{*-})$	$-3.0 \pm 0.9^{+0.12}_{-0.13}$

Table 1: Measurements of $\Sigma_b^{(*)}$ properties. The first uncertainties are statistical, the second uncertainties systematic.

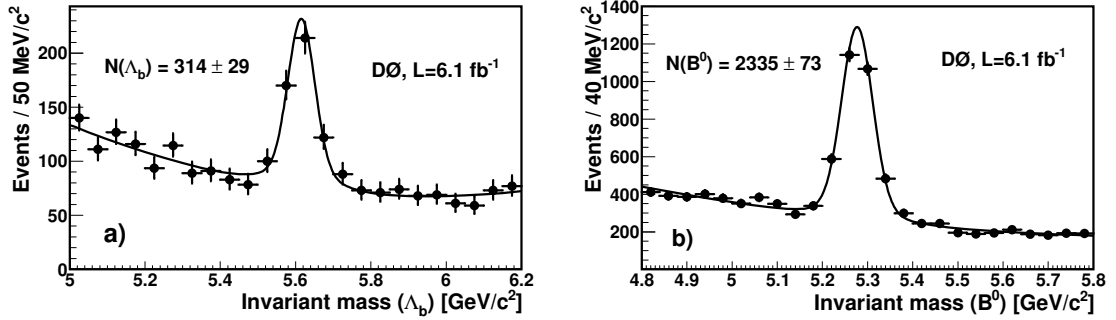


Figure 7: Invariant mass distributions of Λ_b (left) and B^0 (right) candidates.

verify the stability of the result. Using the world average values for the B^0 production and decay fractions, a result of $f(b \rightarrow \Lambda_b) \mathcal{B}(\Lambda_b \rightarrow J/\psi \Lambda) = (6.01 \pm 0.60 \text{ (stat.)} \pm 0.58 \text{ (syst.)} \pm 0.28 \text{ (PDG)}) \times 10^{-5} = (6.01 \pm 0.88) \times 10^{-5}$ is obtained which is about three times more precise than the CDF Run I measurement.

5 Charm Baryons

The Tevatron experiments have not only provided significant contributions on the b baryon sector, but have also collected large samples of charm baryon decays which allow studies at unprecedented precision. The spectrum and decay modes of the $\Sigma_c^{(*)}$ and Λ_c^{*+} states studied by CDF [13] are the same as the ones shown in Fig. 4, but for the charm instead of the b baryon sector.

In a data sample of 5.2 fb^{-1} , $\Lambda_c^+ \rightarrow p K^- \pi^+$ decays are selected by a trigger on displaced tracks. Since charm hadrons have a shorter lifetime than b hadrons, about half of the

triggered Λ_c^+ particles come from b baryon decays. Λ_c^+ candidates are combined with one or two pion tracks to form $\Sigma_c^{(*)}$ or Λ_c^{*+} candidates, respectively. Neural networks are used for the selection of Λ_c^+ , $\Sigma_c^{(*)}$, and Λ_c^{*+} candidates. The networks are trained with data only using the $sPlot$ technique.

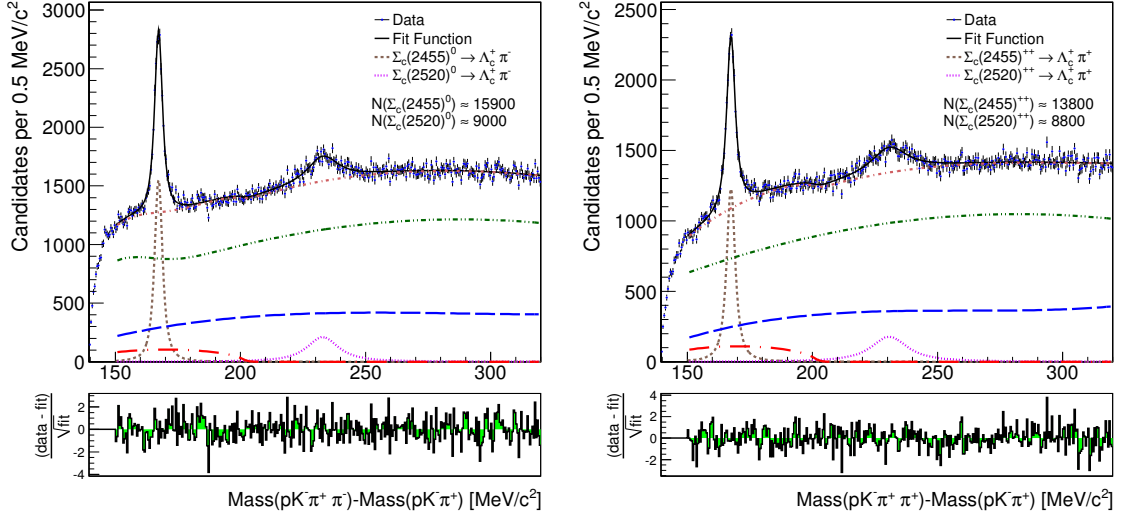


Figure 8: Mass difference distributions of $\Sigma_c^{(*)0}$ (left) and $\Sigma_c^{(*)++}$ (right) candidates.

Distributions of mass differences relative to the reconstructed Λ_c^+ mass are fitted to measure mean masses and widths. The distributions for the $\Sigma_c^{(*)}$ states are shown in Fig. 8. The signals are described by a nonrelativistic Breit-Wigner convolved with a triple Gaussian resolution function. The combinatorial background (green dash-dot-dotted line) is described by a second order polynomial with parameters determined from Λ_c^+ sidebands. In the case of the neutral Σ_c states an additional component from D^* reflections has to be taken into account which is parametrized by a Gaussian. Real Λ_c^+ with a random pion (blue dashed line) are parametrized by a third order polynomial with all parameters free in the fit. The third background component comes from $\Lambda_c^+(2625) \rightarrow \Lambda_c^+ \pi^+ \pi^-$ decays (red dash-dotted line). It is determined using the $\Lambda_c^+(2625)$ yield measured in data. $\Lambda_c^+(2595)$ particles decay mainly resonantly and thus contribute to the signal.

The fit to the mass difference distribution of Λ_c^{*+} candidates is shown in Fig. 9 (right). Signals and backgrounds are treated in the same way as in the fits to the $\Sigma_c^{(*)}$ distributions, except that the cross-feed background now comes from $\Sigma_c^{(*)}$ decays and the threshold effect of $\Lambda_c^{*+}(2595) \rightarrow \Sigma_c \pi$ has to be taken into account. This is done by using a mass dependent width as illustrated in Fig. 9 (left). The parameter determining the width of the lineshape is the pion coupling constant h_2 . CDF has shown that a mass independent width, as used in previous analyses, does not describe the data. Because of the low signal yield in previous

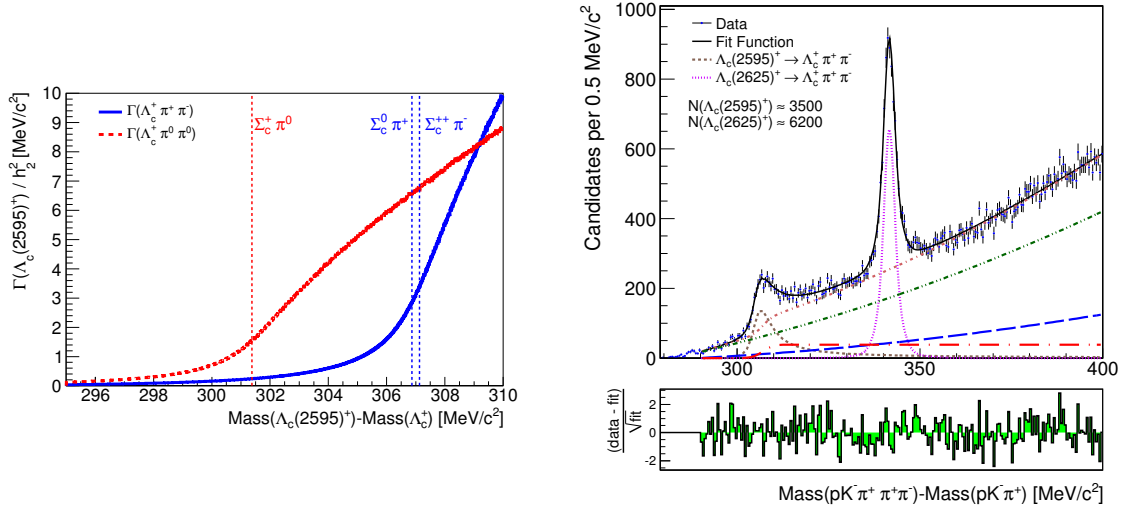


Figure 9: Mass dependent $\Lambda_c^{*+}(2595)$ partial decay widths (left) and mass difference distribution of Λ_c^{*+} candidates (right).

experiments of up to 112 ± 17 events [14], the threshold effect was not observable so far. As a consequence of the threshold effect, the mean $\Lambda_c^{*+}(2595)$ mass is significantly shifted towards lower values.

Numerical results of the measured masses and widths are given in Tab. 2. The $\Sigma_c^{(*)}$ results agree well with the world average values and are of comparable precision. A significant improvement in precision of the Λ_c^{*+} properties and observation of the threshold effect in the $\Lambda_c^{*+}(2595)$ line shape as predicted in Ref. [15] are achieved as illustrated in Fig. 10.

State	Δm [MeV/ c^2]	Γ [MeV/ c^2]
$\Sigma_c(2455)^{++}$	$167.44 \pm 0.04 \pm 0.12$	$2.34 \pm 0.13 \pm 0.45$
$\Sigma_c(2455)^0$	$167.28 \pm 0.03 \pm 0.12$	$1.65 \pm 0.11 \pm 0.49$
$\Sigma_c(2520)^{++}$	$230.73 \pm 0.56 \pm 0.16$	$15.03 \pm 2.12 \pm 1.36$
$\Sigma_c(2520)^0$	$232.88 \pm 0.43 \pm 0.16$	$12.51 \pm 1.82 \pm 1.37$
$\Lambda_c(2595)^+$	$305.79 \pm 0.14 \pm 0.20$	$h_2^2 = 0.36 \pm 0.04 \pm 0.07$
$\Lambda_c(2625)^+$	$341.65 \pm 0.04 \pm 0.12$	< 0.97 at 90% CL

Table 2: Charm baryon properties. The first uncertainties are statistical and the second systematic.

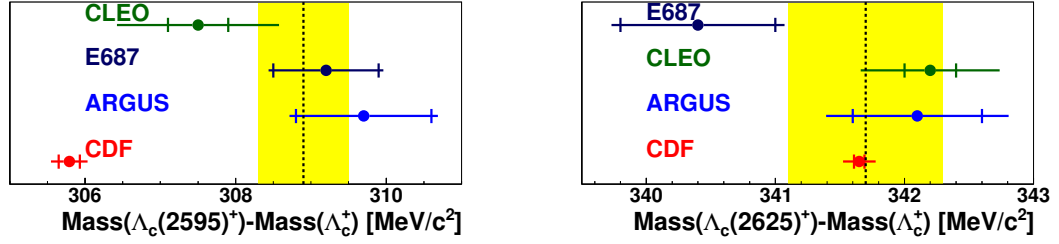


Figure 10: Comparison of Λ_c^{*+} mass difference measurements by CLEO [14], Fermilab E687 [16, 17], ARGUS [18], CDF and the world average without the CDF result (yellow band).

6 Conclusions

So far our knowledge about baryons containing a b quark fits on one page in the PDG particle list table [19]. Thus the observation of new states and improved or even first measurements of heavy baryon properties are very welcome to improve the phenomenological models of strongly bound states and to advance on the way to a deeper understanding of low energy QCD. The Tevatron experiments CDF and D0 have been very active in the last few years and contributed significantly to our knowledge of heavy baryons. With the good performance of the Tevatron both experiments could continue to present new and updated results on this sector as shown in this article.

References

- [1] T. Aaltonen *et al.* (CDF Collaboration), Phys. Rev. Lett. **99**, 202001 (2007).
- [2] V. M. Abazov *et al.* (D0 Collaboration), Phys. Rev. Lett. **99**, 052001 (2007).
- [3] T. Aaltonen *et al.* (CDF Collaboration), Phys. Rev. Lett. **99**, 052002 (2007).
- [4] D. Buskulic *et al.* (ALEPH Collaboration), Phys. Lett. B **384**, 449 (1996).
- [5] P. Abreu *et al.* (DELPHI Collaboration), Z. Phys. C **68**, 541 (1995).
- [6] V. M. Abazov *et al.* (D0 Collaboration), Phys. Rev. Lett. **101**, 232002 (2008).
- [7] T. Aaltonen *et al.* (CDF Collaboration), Phys. Rev. D **80**, 072003 (2009).
- [8] L. Ristori, G. Punz, Annu. Rev. Nucl. Part. Sci. **60**, 595 (2010).
- [9] T. Aaltonen *et al.* (CDF Collaboration), arXiv:1107.4015 [hep-ex].
- [10] CDF Collaboration, CDF note 10286.

- [11] F. Abe *et al.* (CDF Collaboration), Phys. Rev. **D 55**, 1142-1152 (1997).
- [12] V. M. Abazov *et al.* (D0 Collaboration), Phys. Rev. **D 84**, 031102 (2011).
- [13] T. Aaltonen *et al.* (CDF Collaboration), Phys. Rev. **D 84**, 012003 (2011).
- [14] K. W. Edwards *et al.* (CLEO Collaboration), Phys. Rev. Lett. **74**, 3331-3335 (1995).
- [15] A. E. Blechman, A. F. Falk, D. Pirjol, J. M. Yelton, Phys. Rev. **D 67**, 074033 (2003).
- [16] P. L. Frabetti *et al.* (E687 Collaboration), Phys. Rev. Lett. **72**, 961-964 (1994).
- [17] P. L. Frabetti *et al.* (E687 Collaboration), Phys. Lett. **B365**, 461-469 (1996).
- [18] H. Albrecht *et al.* (ARGUS Collaboration), Phys. Lett. **B402**, 207-212 (1997).
- [19] K. Nakamura *et al.* (Particle Data Group Collaboration), J. Phys. G **37**, 075021 (2010).